

RESEARCH ARTICLE

MD simulation of the Tat/Cyclin T1/CDK9 complex revealing the hidden catalytic cavity within the CDK9 molecule upon Tat binding

Kaori Asamitsu¹, Takatsugu Hirokawa^{2,3*}, Takashi Okamoto^{1*}

1 Department of Molecular and Cellular Biology, Nagoya City University Graduate School of Medical Sciences, Nagoya, Aichi, Japan, **2** Molecular Profiling Research Center for Drug Discovery (molprof), National Institute of Advanced Industrial Science and Technology (AIST), Tokyo, Japan, **3** Division of Biomedical Science, Faculty of Medicine, University of Tsukuba, Tsukuba, Ibaraki, Japan

* t-hirokawa@aist.go.jp (TH); tokamoto@med.nagoya-cu.ac.jp (TO)



Abstract

In this study, we applied molecular dynamics (MD) simulation to analyze the dynamic behavior of the Tat/CycT1/CDK9 tri-molecular complex and revealed the structural changes of P-TEFb upon Tat binding. We found that Tat could deliberately change the local flexibility of CycT1. Although the structural coordinates of the H1 and H2 helices did not substantially change, H1', H2', and H3' exhibited significant changes *en masse*. Consequently, the CycT1 residues involved in Tat binding, namely Tat-recognition residues (TRRs), lost their flexibility with the addition of Tat to P-TEFb. In addition, we clarified the structural variation of CDK9 in complex with CycT1 in the presence or absence of Tat. Interestingly, Tat addition significantly reduced the structural variability of the T-loop, thus consolidating the structural integrity of P-TEFb. Finally, we deciphered the formation of the hidden catalytic cavity of CDK9 upon Tat binding. MD simulation revealed that the PITALRE signature sequence of CDK9 flips the inactive kinase cavity of CDK9 into the active form by connecting with Thr186, which is crucial for its activity, thus presumably recruiting the substrate peptide such as the C-terminal domain of RNA pol II. These findings provide vital information for the development of effective novel anti-HIV drugs with CDK9 catalytic activity as the target.

OPEN ACCESS

Citation: Asamitsu K, Hirokawa T, Okamoto T (2017) MD simulation of the Tat/Cyclin T1/CDK9 complex revealing the hidden catalytic cavity within the CDK9 molecule upon Tat binding. PLoS ONE 12(2): e0171727. doi:10.1371/journal.pone.0171727

Editor: Fatah Kashanchi, George Mason University, UNITED STATES

Received: October 18, 2016

Accepted: January 24, 2017

Published: February 8, 2017

Copyright: © 2017 Asamitsu et al. This is an open access article distributed under the terms of the [Creative Commons Attribution License](https://creativecommons.org/licenses/by/4.0/), which permits unrestricted use, distribution, and reproduction in any medium, provided the original author and source are credited.

Data Availability Statement: All relevant data are within the paper and its Supporting Information file.

Funding: This research was partially supported by the Asahi Grass Foundation, the Platform Project for Supporting Drug Discovery and Life Science Research (Platform for Drug Discovery, Informatics, and Structural Life Science) from the Ministry of Education, Culture, Sports, Science, and Technology (MEXT), the Japan Agency for Medical

Introduction

The number of individuals worldwide currently infected with human immunodeficiency virus type 1 (HIV-1) is estimated to be 35.3 million, and the number of deaths due to AIDS continues to rise in spite of effective antiviral agents [1]. Because the major targets of current anti-HIV-1 drugs include viral protease, reverse transcriptase, integrase, and viral attachment, none of which are the rate-determining step of viral replication, the emergence of drug-resistant viral clones due to the high rate of HIV-1 replication is inevitable [2]. Thus, the development of novel anti-HIV-1 therapeutics targeting viral transcription, which is essential for viral replication, remains a pressing need.

Research and Development (AMED) and Junwakai Foundation, Ajuo, Japan.

Competing Interests: The authors have declared that no competing interests exist.

Abbreviations: CDK9, cyclin dependent kinase 9; CycT1, Cyclin T1; HIV-1, human immunodeficiency virus type 1; MD, molecular dynamics; PCA, principal component analysis; P-TEFb, positive transcription elongation factor b; PPI, protein-protein interaction; RMSD, root mean square deviations; RMSF, root mean square fluctuations; TRM, Tat-recognition motif; TRRs, Tat-recognition residues.

Transcription by the HIV-1 provirus is crucially regulated by the virus-encoded transcription factor Tat [3]. Tat requires a cellular transcription factor, positive transcription elongation factor b (P-TEFb), and the viral TAR RNA element formed at the 5'-end of all HIV-1 mRNA transcripts [4,5,6]. It was revealed that P-TEFb contains a regulatory subunit, cyclin T1 (CycT1), and a catalytic subunit, cyclin-dependent kinase 9 (CDK9) [6,7,8], with CycT1 serving as the major interacting protein for Tat [9,10]. In other words, Tat recruits P-TEFb to the nascent viral transcripts, which allows CDK9 to commence the phosphorylation of the C-terminal domain (CTD) of RNA polymerase II (RNAPII), thus stimulating the transcriptional processivity of RNAPII and significantly augmenting viral transcription at the step of elongation [3]. In addition to P-TEFb, a number of transcriptional regulators, such as the superelongation complex [11,12,13,14], Hexim1 [15,16,17], 7SK snRNA [18,19], 7SK snRNP [14,20,21], and the basal transcription machinery [22,23], have been investigated in the context of Tat-mediated HIV transactivation. However, P-TEFb, among others, has long been the most extensively investigated molecular target of HIV transcription.

We and others have previously reported that the functional integrity of the TAR/Tat/P-TEFb complex is crucially involved in the activity of Tat [4,24,25,26]. We demonstrated that the N-terminal cyclin box, together with the Tat-recognition motif (TRM) of CycT1, is involved in Tat-mediated transcriptional activation by directly binding to CDK9 [24]. A number of studies on CycT1 mutants have revealed the distinct roles of various AA residues within CycT1 [25,26,27,28,29], and these findings support the functional integrity of the TAR/Tat/P-TEFb complex. Thus, Tat regulates P-TEFb activity and HIV transcription through a direct protein-protein interaction with CycT1.

In addition, a number of previous studies have demonstrated the regulation of CDK9 activity by a regulatory subunit that was later identified as CycT1 [30,31]. In the context of HIV transcription, Tat is responsible for this CycT1-mediated regulation of CDK9 activity by modulating the action of CycT1 [32]. CDK9 was originally identified as a Tat-associated kinase (TAK) or the cdc-2-like cyclin-dependent kinase PITALRE [33,34,35,36]. The activity of P-TEFb was shown to depend on the phosphorylation of several Ser and Thr residues on CDK9, particularly Thr186 and Ser175 located in the regulatory "T-loop" (amino acids 168–197). It is known that CDK9 T-loop phosphorylation is very low in resting CD4⁺ T-cells [37,38], further limiting P-TEFb activity. Upon T-cell activation, however, the T-loop is heavily phosphorylated, and its conformation changes, thus allowing entry of the substrate and ATP into the CDK9 catalytic pocket [39]. The phosphorylation of Thr186 in the CDK9 T-loop is involved in inducing its catalytic activity and binding to its negative regulator, 7SK snRNP [15,40]. Interestingly, protein phosphatase 1, which dephosphorylates Thr186, is reported to be involved in Tat-mediated transcription [41,42]. Thus, it is assumed that the reversible phosphorylation at Thr186 of CDK9 is critically involved in the regulation of P-TEFb activity [3]. In addition, the phosphorylation of Ser175 in the CDK9 T-loop also plays a regulatory role in altering the competitive binding of Tat to P-TEFb over BRD4 [43,44]. Moreover, the 3D crystal structure of the Tat/CycT1/CDK9 complex has recently been resolved, revealing the physical interaction between Tat and the CDK9 T-loop in addition to its interaction with CycT1 [45].

In order to study the structural background for the catalytic action of P-TEFb, a number of studies have revealed the molecular interaction of Tat and P-TEFb [4,24,25,27,28,46]. However, X-ray crystallography that has been utilized for these studies has generally limited ability in revealing the structural characteristics of protein complex and is considered to have limited chemical space. Since the Tat/P-TEFb complex in such studies utilized the CDK9 molecule with phosphorylated Thr186 that is considered to have regulatory role in its catalytic activity, it is suggested that the molecular flexibility in the vicinity of Thr186 is substantially limited because of the interaction with neighboring Arg residues (Arg 65 and Arg148) [45].

Thus, in this study we have attempted molecular dynamics (MD) simulation in order to search for the transient structure that is “hidden” in the crystallographic studies with the unphosphorylated Thr186 residue of CDK9. Interestingly, MD simulation revealed the dynamic action of proteins [47,48,49]. Toth et al. [49] observed the spontaneous opening and reclosing of the HIV-1 protease flaps based on the NMR structural data. In Filamia et al [50], MD simulation of MAP kinase p38 was able to decipher the hidden intramolecular cavity that fits the effective inhibitor chemical. With regard to the application of MD simulation of protein-protein interaction (PPI), we have recently adopted molecular dynamics (MD) simulation in order to analyze the dynamic characteristics of the Tat-CycT1 protein-protein interaction (PPI) [26]. In addition, Jin et al. [51] also used MD simulation to reveal that HIV-1-Tat binding influences the phosphorylation of the CDK9 T-loop.

Here, we applied MD simulation to analyze the dynamic behavior of the Tat/CycT1/CDK9 tri-molecular complex and revealed the structural changes of P-TEFb upon Tat binding. The results indicate the possible role of Tat in modulating the structural changes of P-TEFb, in particular that of the “catalytic cavity” of CDK9.

Materials and methods

Molecular simulation

MD simulations were carried out using templates of the 3D structures of Tat/P-TEFb (PDBID: 3MI9) and P-TEFb, consisting of CycT1 and CDK9, which were extracted from the same crystal structure of Tat/P-TEFb (3MI9). In order to clarify the structural arrangement of the Tat/P-TEFb complex, the phosphorylated Thr186 in CDK9 within the 3MI9 model was computationally substituted with an unphosphorylated Thr. The Tat sequence in the PDB data (3MI9) was substituted to match the Tat sequence used in our laboratory [25,26,52]: the substituted residues include R7N, K29R, T23N, Q35Y, V36A, I39T, T40R, and A42G (the activities of these Tat molecules are considered nearly identical). Missing side chains, loops, tails, and mutations were built using the homology modeling module in MOE ver.20140901 (Chemical Computing Group Inc.).

The simulation was carried out using the Desmond ver. 3.8 package [53] with the OPLS2005 force field. SGI Rackalbe RP2 Standard-Depth Servers C2108-RP2 (Intel Xeon Processor E5-2670, 16CPU/node) at AIST were used as the computational hardware in this simulation. The initial model structure was refined using the protein preparation wizard in Maestro (Schrödinger, LLC) and placed into TIP3P water molecules solvated with 0.15 M NaCl. After minimization and relaxation of the model, the production molecular dynamics phase was performed for three independent 100-ns simulations in an isothermal-isobaric (NpT) ensemble at 300 K and 1 bar using Langevin dynamics. Long-range electrostatic interactions were computed using the Smooth Particle Mesh Ewald method. All system setups were performed using Maestro. Trajectory coordinates were recorded every 100 ps. The simulation trajectories were then analyzed for the sampled conformations in all structural models. The obtained trajectory was processed utilizing the AMBER11 tool ptraj for the calculations of RMSD and PMSF for protein RMSD. All molecular figures were generated using PyMOL (Schrödinger, LLC).

Principal Component Analysis (PCA)

Principal component analysis (PCA) was performed on the 3D coordinates of C α atoms of the TRRs [26] of CycT1 for MD trajectories of Tat/CycT1/CDK9 and CycT1/CDK9 complexes. The PCA results for the Tat/CycT1/CDK9 and CycT1/CDK9 complex structures were analyzed, and the conformational differences were visualized by plotting to the PC1 (primary component 1) and PC2 axes. PCA is a standard statistical method routinely used to identify

variable correlations in a system from atomic fluctuations in an MD trajectory. The RMSD distance matrix of TRR C α atoms for the combined trajectories of Tat/CycT1/CDK9 and CycT1/CDK9 structures was calculated after structure alignment of all C α atoms to prepare the input matrix to PCA. PCA was performed using R (version 3.1.1.), which is a software language and environment for statistical computing and graphics.

Concavity shape analysis of the protein structure

The likeliest active site pocket around the ATP-binding position and Thr186 within the representative structure from the MD simulations was identified using the SiteFinder module of MOE. The shape of the active site pocket was represented by small dummy atoms (α -spheres). The representative structures of Tat/P-TEFb and P-TEFb were each chosen from 3,000 trajectory coordinates (1,000 trajectories each for three independent run) by a k-means clustering algorithm ($k = 1$) using the AMBER11 tool ptraj command.

Results

MD simulations of the Tat/CycT1/CDK9 trimolecular and CycT1/CDK9 bimolecular complexes

The dynamic structural fluctuations of P-TEFb in the presence or the absence of Tat were analyzed by MD simulation for 100 ns. The structural fluctuation of the Tat/CycT1/CDK9 trimolecular complex (3MI9) was analyzed using Desmond ver. 3.8 as described in Experimental Procedures for 100 ns (Fig 1, left panel). The fluctuation of the CycT1/CDK9 bi-molecular structure was similarly examined using the coordinates of 3MI9 without the Tat protein moiety as the starting structure (Fig 1, right panel). In both MD simulations, the plateau was reached after approximately 30–50 ns. Similar computations were repeated three times, and similar results were obtained within the limited variations. Although the addition of Tat did not significantly change the mean of the root mean square deviation (RMSD) value of C α positions of Tat/CycT1/CDK9, it apparently reduced its variation, suggesting that Tat might restrict the structural fluctuation of CycT1/CDK9 complex.

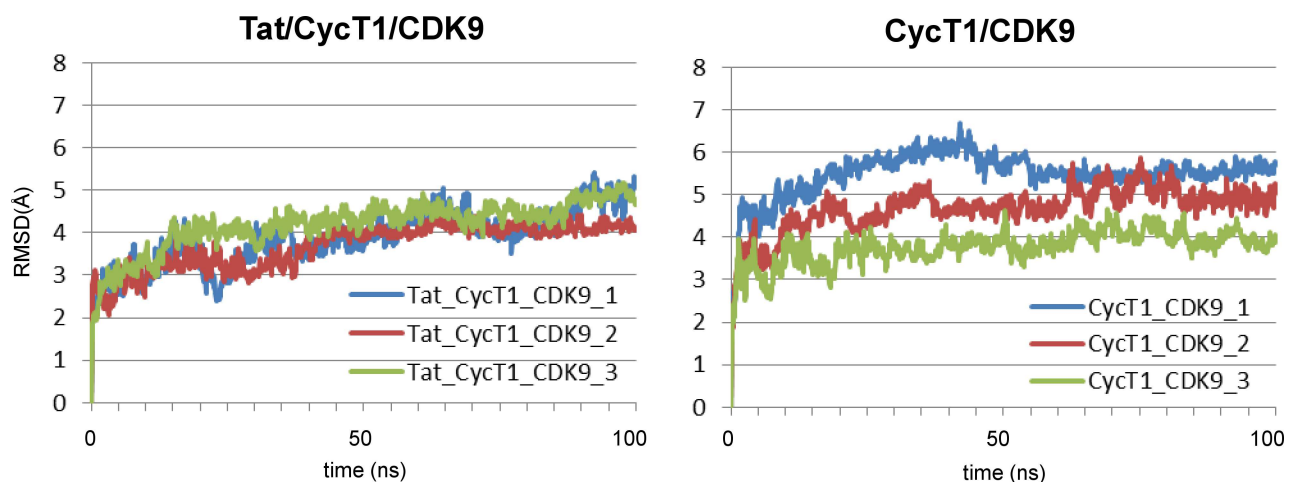


Fig 1. Molecular dynamics (MD) simulation. The time dependence of the root mean square deviations (RMSDs) of C α atoms of Tat/CycT1/CDK9 (left) and CycT1/CDK9 (right) in the 100-ns MD simulations. For each complex, the results of three independent computations are shown (1, 2, and 3, for each complex).

doi:10.1371/journal.pone.0171727.g001

Comparison of Root Mean Square Fluctuations (RMSFs) of the CycT1 molecule within the tri- and bi-molecular complexes upon MD simulation

As shown in Fig 2A, we determined whether Tat could change the local flexibility of CycT1. As shown in the left panel, we found that the AA residues at 117S, 122R, and 217D were relatively flexible within the CycT1 molecule aligned with the original CycT1 (using the 3MI9 structure before MD simulation). The flexibility of these AAs did not significantly change in the presence or absence of Tat (compare the red and blue lines). Interestingly, the CycT1 region spanning from 146 to 217AA was continuously shifted when the CDK9 coordinate was used as the reference (Fig 2A, right panel). This structural shift was reduced when Tat was present, thus confirming the results of Fig 1. The H1'-H2'-H3' region contained within the AA region spanning from 146 to 217 described above was located in the Tat-binding pocket that is formed together with the H1 and H2 helices. Although the structural coordinates of the H1 and H2 helices did not substantially change, those of H1', H2', and H3' exhibited significant changes *en masse*. It was remarkable that the structural coordinate of the H3' helix was also shifted although Tat directly interacts with the H1, H2, H1', and H2' helices but not the H3' helix. These findings also indicated the rotation of CycT1 relative to CDK9, which will be discussed later.

We previously identified the amino acid residues on CycT1, termed "Tat recognition residues (TRRs)" [26], involved in the interaction between Tat and CycT1. As shown in Fig 2B, RMSF values of those AA residues involved in Tat binding, or TRRs, were not significantly changed irrespective of the presence of Tat. However, when only the coordinates of these AA residues were statistically examined by PCA (Fig 2C), these coordinates of TRRs in the absence of Tat were classified into multiple distinct groups, suggesting the flexibility of the CycT1 structure before Tat-binding. Interestingly, the addition of Tat to P-TEFb dramatically reduced this flexibility, leaving one major group (Fig 2C, compare the left and the right panels).

Stabilization of the CDK9 T-loop by Tat

As shown in Fig 3, we examined the structural variation of CDK9 in complex with CycT1 in the presence or absence of Tat using the original CDK9 and CycT1 coordinates as the reference. Interestingly, Tat addition appeared to reduce the variability of the T-loop containing the Ser175 and Thr186 residues in CDK9 that are phosphorylated upon its activation (Fig 3, lower panels), although the other part of this molecule was not significantly affected. When the CycT1 structure was used as the structural reference, Tat binding similarly reduced the structural variability of the T-loop (Fig 3, right panel). It was assumed that this stabilization was due to the geometrical proximity of Tat and the CDK9 T-loop, which was considered crucial for the continuous phosphorylation of these residues.

Comparison of the 3D structures of P-TEFb with or without Tat

The MD simulation results indicated the Tat-induced structural changes of P-TEFb. In Fig 4A and 4B, we superimposed the CycT1 structure in the presence (cyan) or absence (orange) of Tat. We found a narrowing of the Tat-binding cleft, formed between the H1-H2 and H1'-H2'-(H3') helices, upon Tat binding (compare the upper and bottom figures in Fig 4A). MD simulation revealed that this narrowing was induced by the internal shift of the H1' and H2' helices to the CycT1 core (compare the orange helices with the cyan helices in Fig 4A). We previously reported the internal movement of these helices upon MD simulation of only CycT1 molecule [26]. It was thus hypothesized that this internal movement might be crucial for Tat binding and the structural stabilization of the complex. When the CycT1/CDK9 complex was superimposed

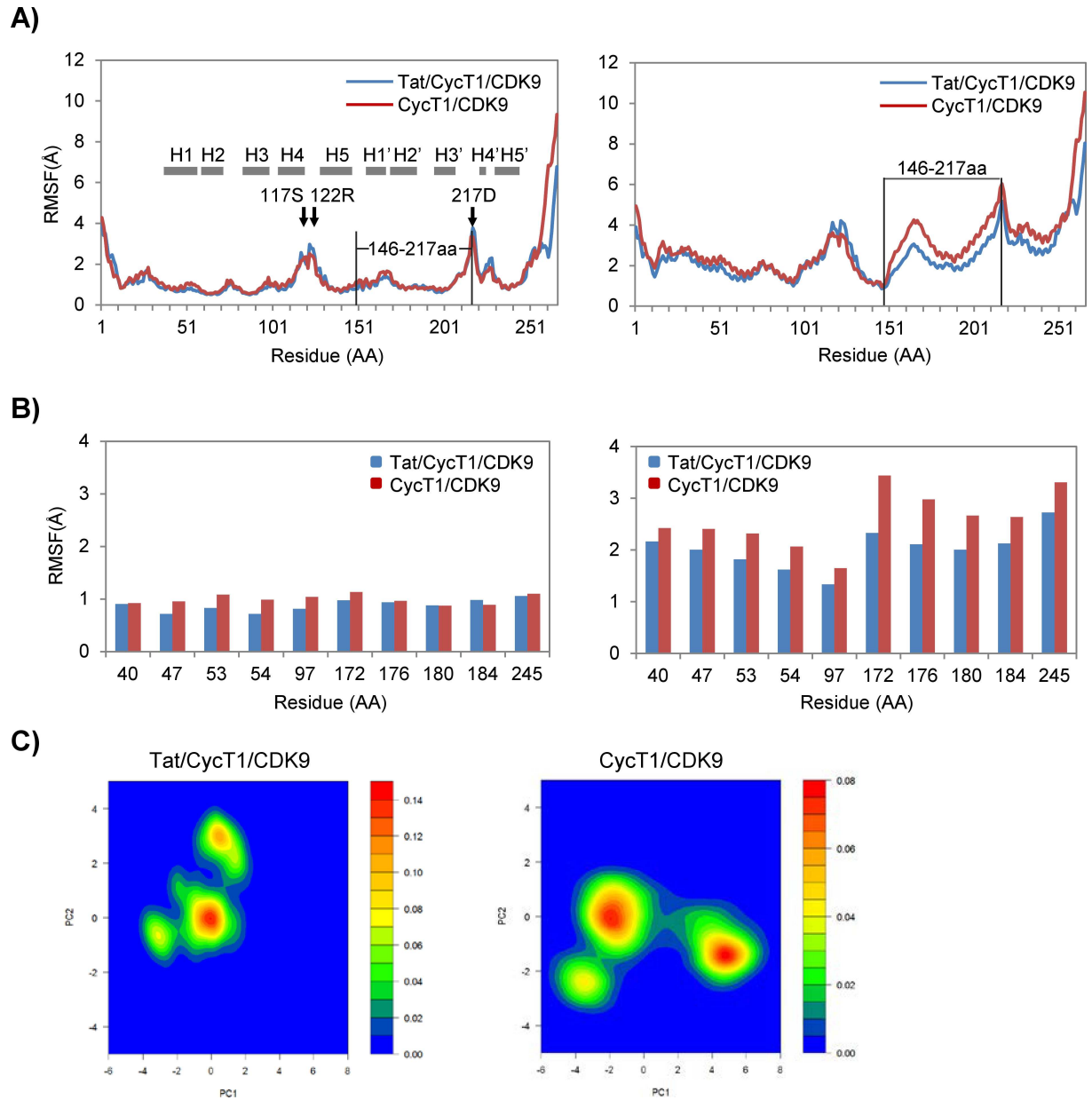


Fig 2. Tat restricts possible structural fluctuations of the CycT1/CDK9 complex. (A) RMSFs of CycT1 molecules (1–266 AA) during a 100-ns MD simulation of the Tat/CycT1/CDK9 (blue) and CycT1/CDK9 (red) complexes. Averages of three independent computations for each complex are shown. RMSF values of C α atoms of CycT1 aligned to the initial coordinate of CycT1 are shown on the left; those using the initial coordinates of CDK9 for alignment are shown on the right. The locations of the α -helices are as follows (gray bars): H1, 31-52AA; H2, 54-69AA; H3, 80-64AA; H4, 101-102AA; H5, 125-143AA; H1', 153-163AA; H2', 168-184AA; H3', 193-207AA; H4', 221-224AA; and H5', 231-245AA. The positions of 117S, 122R, and 217D are indicated by black arrows. (B) Plots of RMSF values of CycT1 TRRs. RMSFs aligned with CycT1 (initial) and those aligned with CDK9 (initial) are shown on the left and the right, respectively. (C) Two-dimensional PCA projections of trajectories for the CycT1 TRRs obtained from the above MD simulations. The C α coordinates for TRRs are plotted over PCA axes with principal component 1 and 2 (PC1 and PC2). The definition of the PCA axes was based on PCA calculations of all C α coordinates with all CycT1 models, including Tat/CycT1/CDK9 and CycT1/CDK9. Using the RMSD distance data for only the TRR C α atoms, each trajectory data set was plotted in accordance with PC1 and PC2 for the abscissa and ordinate, respectively. The 2D (PC1-PC2) plots of all 1,000 trajectories obtained from each triplicated MD simulation with Tat/CycT1/CDK9 (left) and CycT1/CDK9 (right) are shown. The probability distribution (in color) of the MD trajectories based on PCA was estimated using the kernel density estimation method in R version 3.1.1.

doi:10.1371/journal.pone.0171727.g002

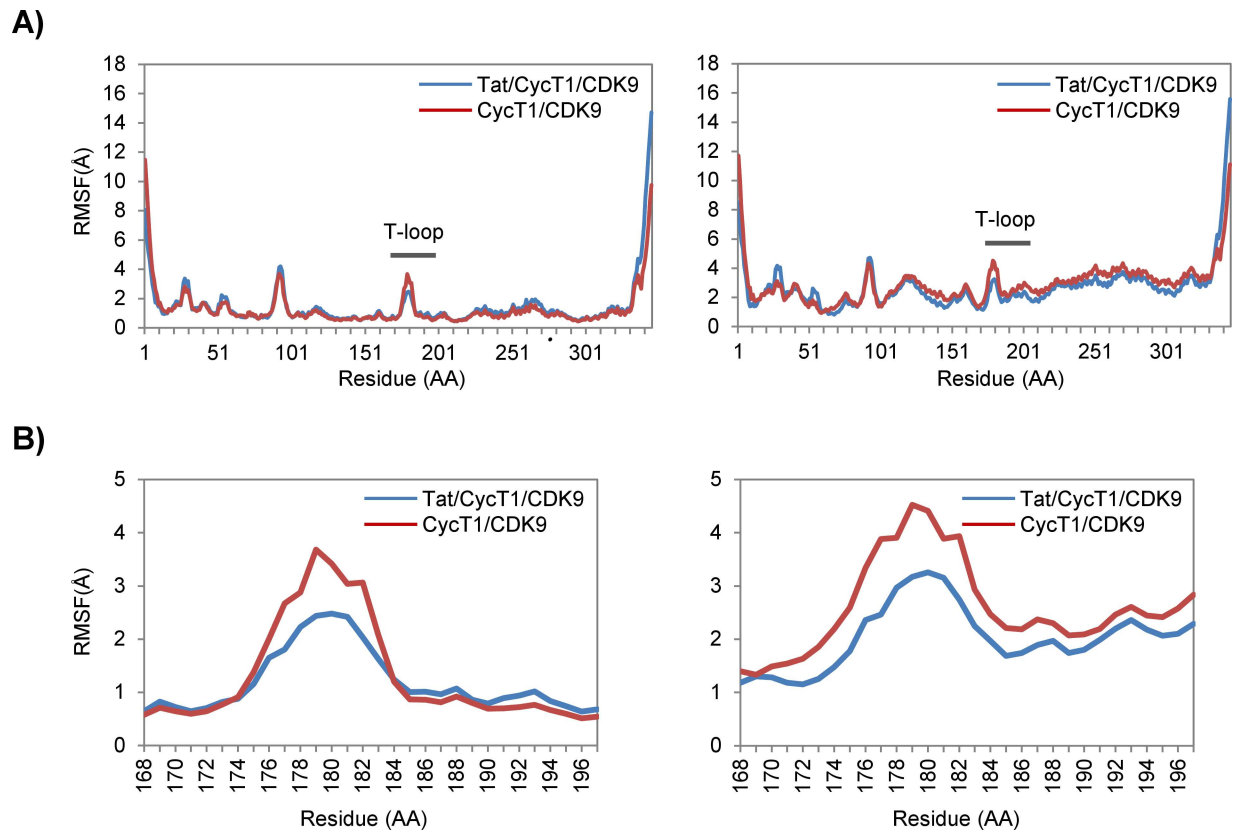


Fig 3. Tat restricts the possible structural fluctuations of the CDK9 T-loop. RMSFs of CDK9 molecules (1–345 AA) (A) and the CDK9 T-loop (168–197 AA) (B) during a 100-ns MD simulation of the Tat/CycT1/CDK9 (blue) and CycT1/CDK9 (red) complexes. Averages of three independent computations for each complex are shown. RMSFs of C α atoms of CDK9 aligned with the initial coordinate of CDK9 are shown on the left. Those with the initial coordinates of CycT1 are shown on the right.

doi:10.1371/journal.pone.0171727.g003

on CycT1, the CDK9 molecule appeared to rotate 5° (Fig 4B). This molecular rotation was previously reported by Tahirov et al. [45], thus corroborating our current MD simulation analyses.

As shown in Fig 4C and 4D, we analyzed the CDK9 structure in the presence (dark green) or absence (light green) of Tat. The T-loop appeared to shift away from Tat (Fig 4C). When the structure of the CycT1 molecule was assessed together (Fig 4D), only one AA, Phe146 of CycT1, stayed in the same position (also refer to Fig 2A, right panel). In contrast, the positions of AA residues between 147E and 217D were quite variable. The molecular rotation of CycT1 appeared to surround F146, which is located in the middle of 10 α -helices of CycT1, with the H1-H5 and H1'-H5' helices.

Tat-induced stabilization of the CycT1/CDK9 complex

Fig 5 illustrates the atomic details of the principal interactions between CycT1 and CDK9 in the presence or absence of Tat. In contrast to the absence of Tat, Tat significantly increased the number of hydrogen bonds between these two molecules (from 5 to 11 hydrogen bonds; see the details in S1 Table). Thus, Tat stabilizes the CycT1/CDK9 complex by creating a significant number of novel hydrogen bonds. With regard to hydrophobic interactions in the CycT1/CDK9 complex, the addition of the Tat molecule appears to endow hydrophobic interactions in a more localized fashion. These findings indicate the molecular basis of Tat's action to stabilize the CycT1/CDK9 complex. S1 Table summarizes the molecular details of the hydrogen

bonding and hydrophobic interactions between CycT1 and CDK9 induced by Tat binding. Consistent with this finding from the MD simulation, we have previously reported that Tat induces increased binding affinity between CycT1 and CDK9 using image-based protein-protein interaction analysis in live cells [52].

Induction of catalytic cavity within CDK9 by Tat alongside the PITALRE signature sequence

The substrate specificity of CDK9 has been shown to be determined by the PITALRE sequence [33]. In order to analyze the effects of Tat, we applied MD simulation to analyze the molecular

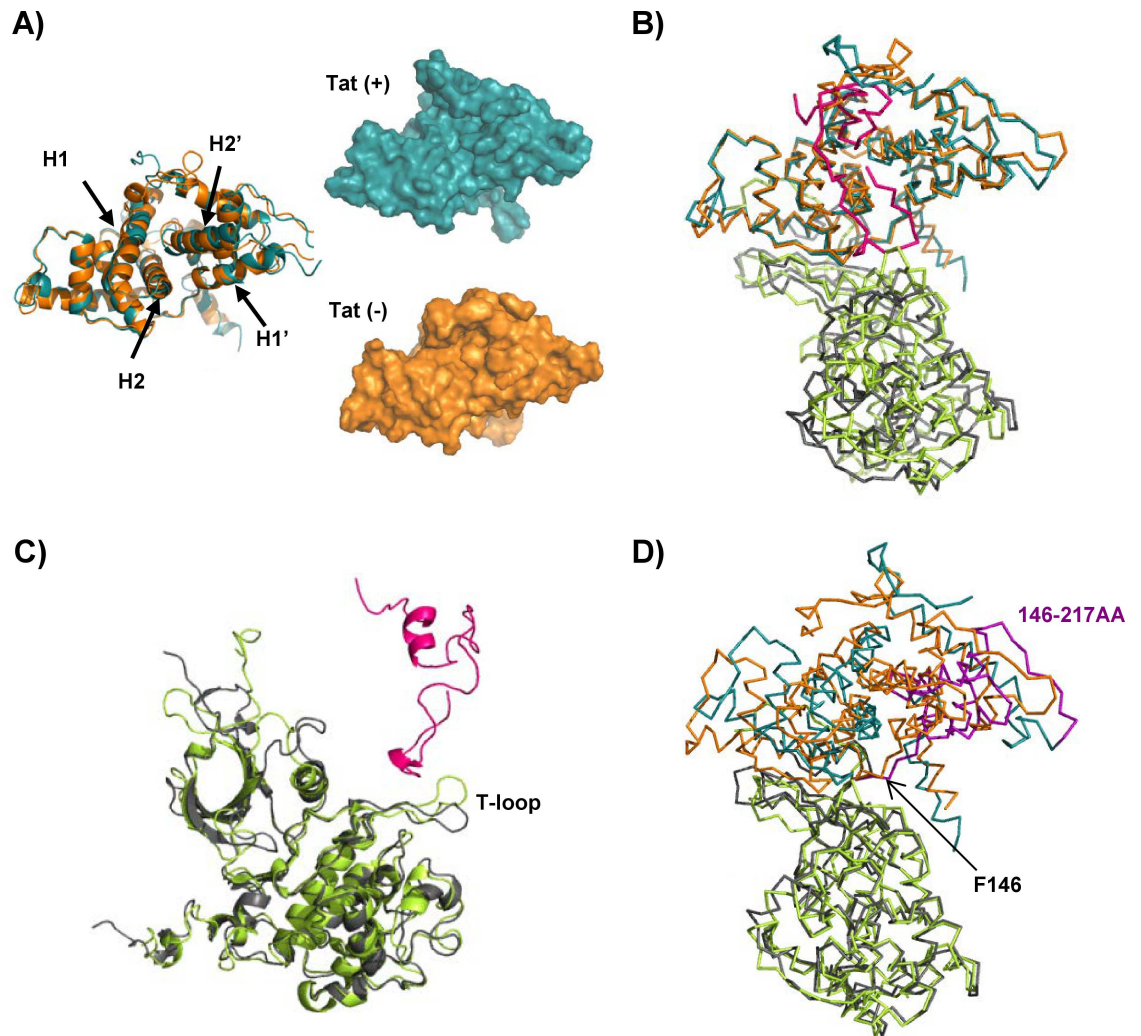


Fig 4. Comparison of the representative structures of the Tat/CycT1/CDK9 and CycT1/CDK9 models obtained by MD simulation. (A) Comparison of the depicted CycT1 structures observed for the Tat/CycT1/CDK9 (cyan) and CycT1/CDK9 (orange) complexes. Note that the cleft formed with the H1-H2 and H1'-H2' helices narrowed following Tat binding. Left, the superimposed CycT1 models; right, the surface representations of CycT1 molecules with (cyan) or without (orange) Tat. (B) Superimposition of CycT1. Tat/CycT1/CDK9: Tat (magenta), CycT1 (cyan), and CDK9 (dark green); CycT1/CDK9: CycT1 (orange) and CDK9 (light green). Note the rotation of CDK9 (see details in the text). (C) Superimposition of CDK9 showing the T-loop shift induced by Tat binding. (D) Superimposition of CDK9 showing the rotation of CycT1. Note that F146 of CycT1 stayed in the same position with or without Tat. The colors in C and D are the same as in B. The representative structures were each chosen from 3,000 trajectory coordinates (1,000 trajectories each for three independent runs) by the k-means clustering algorithm ($k = 1$) using the AMBER11 tool ptraj command.

doi:10.1371/journal.pone.0171727.g004

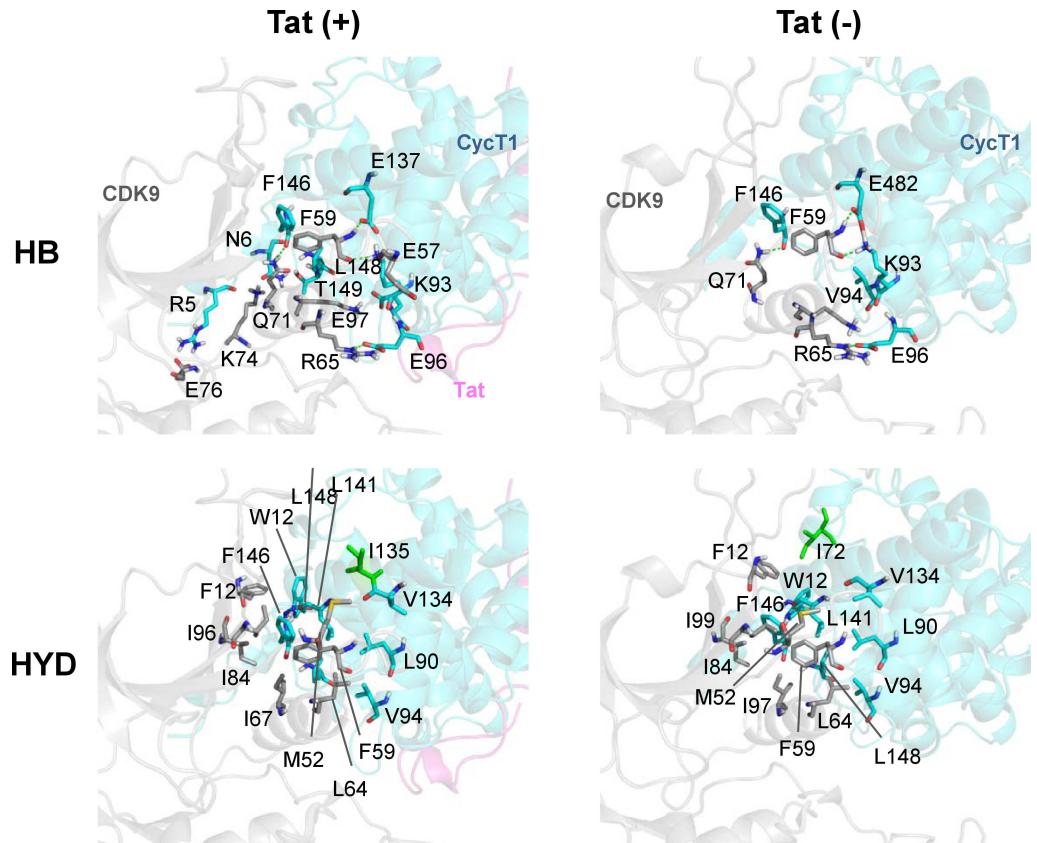


Fig 5. Atomic details of the principal interactions between CycT1 and CDK9 in the presence or absence of Tat. In order to identify the directly interacting residues, Contact Analyzer software (MOE ver. 20140910) was utilized. CDK9 is shown as a light gray ribbon with gray sticks, and CycT1 is shown as a light cyan ribbon with cyan sticks; the residues involved in hydrogen or hydrophobic bonds are depicted. Tat is shown as a light pink ribbon. The CycT1 residues affected by Tat binding through hydrophobic interactions are labeled in green. HB, hydrogen bond; HYD, hydrophobic interaction.

doi:10.1371/journal.pone.0171727.g005

remodeling of the CycT1/CDK9 complex induced by Tat. As shown in Fig 6, Thr186 is located within the catalytic center of CDK9 [15,40,45] adjacent to PITALRE and the catalytic cavity (drawn in yellow) whose structure is not continuous with Thr186 (Fig 5, right panel). The addition of Tat appears to induce the interconnection of two internal Arg residues of CDK9, Arg65 and Arg148, with Thr186, thus forming a continuous catalytic cavity that links Thr186 and the substrate ATP molecule. It appears that the PITALRE signature sequence flips the vacant kinase cavity (left panel) to become connected with Thr186 (right panel), thus presumably recruiting the substrate peptide such as the C-terminal domain of RNA pol II (not shown in the figure). The liberated pyrophosphate (PP_i; red) moiety from ATP might move through the continuous catalytic cavity to target the substrate.

Discussion

It has been proposed that HIV-specific transcriptional regulation could be an ideal target for an effective AIDS therapy, as it would block the rate-determining step of viral replication and prevent the generation of drug-resistant viral clones [54]. In this study, we analyzed the dynamic molecular behavior of Tat during the activation of the host transcription elongation factor P-TEFb by applying MD simulation to clarify the dynamic structural changes of CycT1

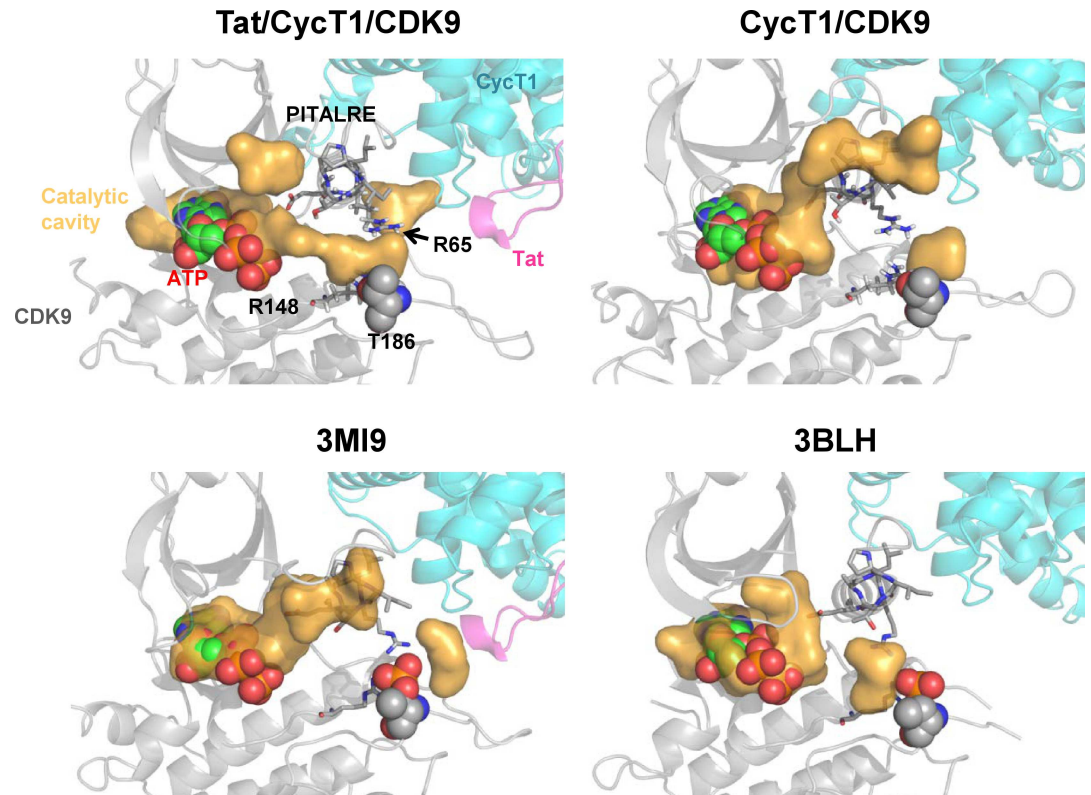


Fig 6. Induction of continuous catalytic cavity within the CDK9 molecule by Tat. CDK9, CycT1, and Tat are shown as gray, cyan, and pink ribbons, respectively. ATP is shown as a sphere with carbon atoms colored green, nitrogen atoms colored blue, oxygen atoms colored red, and phosphate atoms colored orange. The proposed ATP position was located in the binding site of CDK9 by structural alignment with the crystal structure of ATP-bound CDK9 (PDB ID: 3MIA). Thr186 is shown as spheres. The side chains of Arg85 and Arg148 in CDK9 are shown as sticks. The CDK9 catalytic cavity is shown in orange. Note the formation of a continuous catalytic cavity alongside the signature PITALRE sequence within the CDK9 molecule. The locations of cavities depicted in previous crystallographic analyses (3MI9 and 3BLH, corresponding to the Tat/CycT1/CDK9 and CycT1/CDK9 complexes, respectively) are presented below.

doi:10.1371/journal.pone.0171727.g006

and CDK9 upon binding to Tat. We observed that Tat binds to the CycT1 cleft that is formed by two sets of α -helices, namely the H1-H2 and H1'-H2'-H3' helices, thus confirming the initial finding by Tahirov et al. [45]. Interestingly, we also found that upon Tat binding, this cleft is narrowed by primarily shifting the H1'-H2'-H3' helices. More importantly, our MD simulation reveals, for the first time, that the accumulation of these subtle structural changes culminated in the formation of a continuous catalytic cavity that links the kinase substrate ATP to the CDK9 Thr186 that is located at its catalytic center alongside the signature sequence PITALRE [15,39].

In the present study, we found that the CycT1 H1'-H2'-H3' helices lost flexibility in the presence of Tat, thus stabilizing the Tat/CycT1 complex. In the absence of Tat, the H1'-H2'-H3' helices relatively opened up, with Phe146 as the symmetric center of this movement. We have previously reported that the flexibility of the H1' and H2' helices of CycT1 was crucial for the Tat-mediated transcriptional activation of HIV-1 in a study in which we analyzed the effects of the substitution of crucial AA residues [26]. We also proposed a pre-existing model where the putative Tat-binding pocket is transcendently present on the molecular surface of CycT1, which was confirmed by the present MD simulation [26,55]. As shown in Fig 2C, Tat

appears to choose one principal structure conformed by TRRs, whereas there are three possible structures for the TRRs in the absence of Tat.

More importantly, we observed the loss of flexibility of the CDK9 T-loop in the presence of Tat (Fig 3). Tat appears to restrict the flexible movement of the T-loop structure (Fig 4C). This leads to the formation of a continuous catalytic cavity that could liberate PPi from ATP to attack Thr186 through two Arg residues (Arg65 and Arg148) and then eventually the target C-terminal domain (CTD) of RNA polymerase II. It remains to be clarified whether the CTD moiety could actually be brought close to the Tat/CycT1/CDK9 complex upon co-crystallization. It is expected that the CDK9 catalytic center could be located in close proximity to the Ser2 residue within the CTD heptad sequence. Furthermore, the role of the signature sequence PITALRE could be to act as a fulcrum for the trans-generation of the catalytic cavity.

Our current MD simulation revealed a +5° rotation of CDK9, which was consistent with a previous report by Tahirov et al. [45], although they could not demonstrate the continuous structural extension of the catalytic cavity. This suggests the transient formation of such a cavity upon the dynamic movement of the CycT1/CDK9 complex in the presence of Tat. It is noted that this structural change of P-TEFb might be rather specific for Tat because other transcriptional activators such as AFF4 do not involve CDK9 kinase activity [56].

These findings should provide the structural basis for the development of a Tat-specific inhibitor that can not only inhibit the explosive replication capability of HIV but also prevent the rapid emergence of viral clones resistant to conventional anti-HIV regimens. Further studies are needed to clarify the details of the target structure against which novel anti-Tat compounds should be developed.

Supporting information

S1 Table. Inter and intra-helical hydrogen bonds within Tat/CycT1/CDK9 and CycT1/CDK9 representative structures.
(DOCX)

Author contributions

Conceptualization: KA TO.

Data curation: KA TH TO.

Formal analysis: KA TH TO.

Funding acquisition: KA TH TO.

Investigation: KA TO TH.

Methodology: KA TH TO.

Project administration: TO TH.

Resources: KA TH TO.

Software: KA TH.

Supervision: TO.

Validation: KA TH TO.

Visualization: KA TH TO.

Writing – original draft: KA TO.

Writing – review & editing: KA TH TO.

References

1. Joint United Nations Programme on HIV/AIDS (UNAIDS), Global Report: UNAIDS report on the global AIDS epidemic 2013, 2013. (see http://www.unaids.org/en/media/unaids/contentassets/documents/epidemiology/2013/gr2013/UNAIDS_Global_Report_2013_en.pdf)
2. Deeks SG, Autran B, Berkhout B, Benkirane M, Cairns S, Chomont N, et al. (2012) Towards an HIV cure: a global scientific strategy. *Nat Rev Immunol* 12: 607–614. doi: [10.1038/nri3262](https://doi.org/10.1038/nri3262) PMID: [22814509](https://pubmed.ncbi.nlm.nih.gov/22814509/)
3. Ott M, Geyer M, Zhou Q (2011) The control of HIV transcription: keeping RNA polymerase II on track. *Cell Host Microbe* 10: 426–435. doi: [10.1016/j.chom.2011.11.002](https://doi.org/10.1016/j.chom.2011.11.002) PMID: [22100159](https://pubmed.ncbi.nlm.nih.gov/22100159/)
4. Garber ME, Wei P, Jones KA (1998) HIV-1 Tat interacts with cyclin T1 to direct the P-TEFb CTD kinase complex to TAR RNA. *Cold Spring Harb Symp Quant Biol* 63: 371–380. PMID: [10384302](https://pubmed.ncbi.nlm.nih.gov/10384302/)
5. Wei P, Garber ME, Fang SM, Fischer WH, Jones KA (1998) A novel CDK9-associated C-type cyclin interacts directly with HIV-1 Tat and mediates its high-affinity, loop-specific binding to TAR RNA. *Cell* 92: 451–462. PMID: [9491887](https://pubmed.ncbi.nlm.nih.gov/9491887/)
6. Peterlin BM, Price DH (2006) Controlling the elongation phase of transcription with P-TEFb. *Mol Cell* 23: 297–305. doi: [10.1016/j.molcel.2006.06.014](https://doi.org/10.1016/j.molcel.2006.06.014) PMID: [16885020](https://pubmed.ncbi.nlm.nih.gov/16885020/)
7. Bieniasz PD, Grdina TA, Bogerd HP, Cullen BR (1998) Recruitment of a protein complex containing Tat and cyclin T1 to TAR governs the species specificity of HIV-1 Tat. *EMBO J* 17: 7056–7065. doi: [10.1093/emboj/17.23.7056](https://doi.org/10.1093/emboj/17.23.7056) PMID: [9843510](https://pubmed.ncbi.nlm.nih.gov/9843510/)
8. Fujinaga K, Taube R, Wimmer J, Cujec TP, Peterlin BM (1999) Interactions between human cyclin T, Tat, and the transactivation response element (TAR) are disrupted by a cysteine to tyrosine substitution found in mouse cyclin T. *Proc Natl Acad Sci U S A* 96: 1285–1290. PMID: [9990016](https://pubmed.ncbi.nlm.nih.gov/9990016/)
9. Marshall NF, Peng J, Xie Z, Price DH (1996) Control of RNA polymerase II elongation potential by a novel carboxyl-terminal domain kinase. *J Biol Chem* 271: 27176–27183. PMID: [8900211](https://pubmed.ncbi.nlm.nih.gov/8900211/)
10. Peng J, Zhu Y, Milton JT, Price DH (1998) Identification of multiple cyclin subunits of human P-TEFb. *Genes Dev* 12: 755–762. PMID: [9499409](https://pubmed.ncbi.nlm.nih.gov/9499409/)
11. He N, Chan CK, Sobhian B, Chou S, Xue Y, Liu M, et al. (2011) Human Polymerase-Associated Factor complex (PAFc) connects the Super Elongation Complex (SEC) to RNA polymerase II on chromatin. *Proc Natl Acad Sci U S A* 108: E636–645. doi: [10.1073/pnas.1107107108](https://doi.org/10.1073/pnas.1107107108) PMID: [21873227](https://pubmed.ncbi.nlm.nih.gov/21873227/)
12. He N, Liu M, Hsu J, Xue Y, Chou S, Burlingame A, et al. (2010) HIV-1 Tat and host AFF4 recruit two transcription elongation factors into a bifunctional complex for coordinated activation of HIV-1 transcription. *Mol Cell* 38: 428–438. doi: [10.1016/j.molcel.2010.04.013](https://doi.org/10.1016/j.molcel.2010.04.013) PMID: [20471948](https://pubmed.ncbi.nlm.nih.gov/20471948/)
13. Smith E, Lin C, Shilatifard A (2011) The super elongation complex (SEC) and MLL in development and disease. *Genes Dev* 25: 661–672. doi: [10.1101/gad.2015411](https://doi.org/10.1101/gad.2015411) PMID: [21460034](https://pubmed.ncbi.nlm.nih.gov/21460034/)
14. Sobhian B, Laguette N, Yatim A, Nakamura M, Levy Y, Kiernan R, et al. (2010) HIV-1 Tat assembles a multifunctional transcription elongation complex and stably associates with the 7SK snRNP. *Mol Cell* 38: 439–451. doi: [10.1016/j.molcel.2010.04.012](https://doi.org/10.1016/j.molcel.2010.04.012) PMID: [20471949](https://pubmed.ncbi.nlm.nih.gov/20471949/)
15. Li Q, Price JP, Byers SA, Cheng D, Peng J, Price DH (2005) Analysis of the large inactive P-TEFb complex indicates that it contains one 7SK molecule, a dimer of HEXIM1 or HEXIM2, and two P-TEFb molecules containing Cdk9 phosphorylated at threonine 186. *J Biol Chem* 280: 28819–28826. doi: [10.1074/jbc.M502712200](https://doi.org/10.1074/jbc.M502712200) PMID: [15965233](https://pubmed.ncbi.nlm.nih.gov/15965233/)
16. Michels AA, Fraldi A, Li Q, Adamson TE, Bonnet F, Nguyen VT, et al. (2004) Binding of the 7SK snRNA turns the HEXIM1 protein into a P-TEFb (CDK9/cyclin T) inhibitor. *EMBO J* 23: 2608–2619. doi: [10.1038/sj.emboj.7600275](https://doi.org/10.1038/sj.emboj.7600275) PMID: [15201869](https://pubmed.ncbi.nlm.nih.gov/15201869/)
17. Sedore SC, Byers SA, Biglione S, Price JP, Maury WJ, Price DH (2007) Manipulation of P-TEFb control machinery by HIV: recruitment of P-TEFb from the large form by Tat and binding of HEXIM1 to TAR. *Nucleic Acids Res* 35: 4347–4358. doi: [10.1093/nar/gkm443](https://doi.org/10.1093/nar/gkm443) PMID: [17576689](https://pubmed.ncbi.nlm.nih.gov/17576689/)
18. Nguyen VT, Kiss T, Michels AA, Bensaude O (2001) 7SK small nuclear RNA binds to and inhibits the activity of CDK9/cyclin T complexes. *Nature* 414: 322–325. doi: [10.1038/35104581](https://doi.org/10.1038/35104581) PMID: [11713533](https://pubmed.ncbi.nlm.nih.gov/11713533/)
19. Yang Z, Zhu Q, Luo K, Zhou Q (2001) The 7SK small nuclear RNA inhibits the CDK9/cyclin T1 kinase to control transcription. *Nature* 414: 317–322. doi: [10.1038/35104575](https://doi.org/10.1038/35104575) PMID: [11713532](https://pubmed.ncbi.nlm.nih.gov/11713532/)
20. D'Orso I, Frankel AD (2010) RNA-mediated displacement of an inhibitory snRNP complex activates transcription elongation. *Nat Struct Mol Biol* 17: 815–821. doi: [10.1038/nsmb.1827](https://doi.org/10.1038/nsmb.1827) PMID: [20562857](https://pubmed.ncbi.nlm.nih.gov/20562857/)
21. Muniz L, Egloff S, Ughy B, Jady BE, Kiss T (2010) Controlling cellular P-TEFb activity by the HIV-1 transcriptional transactivator Tat. *PLoS Pathog* 6: e1001152. doi: [10.1371/journal.ppat.1001152](https://doi.org/10.1371/journal.ppat.1001152) PMID: [20976203](https://pubmed.ncbi.nlm.nih.gov/20976203/)

22. Raha T, Cheng SW, Green MR (2005) HIV-1 Tat stimulates transcription complex assembly through recruitment of TBP in the absence of TAFs. *PLoS Biol* 3: e44. doi: [10.1371/journal.pbio.0030044](https://doi.org/10.1371/journal.pbio.0030044) PMID: [15719058](https://pubmed.ncbi.nlm.nih.gov/15719058/)
23. Sikorski TW, Buratowski S (2009) The basal initiation machinery: beyond the general transcription factors. *Curr Opin Cell Biol* 21: 344–351. doi: [10.1016/j.ceb.2009.03.006](https://doi.org/10.1016/j.ceb.2009.03.006) PMID: [19411170](https://pubmed.ncbi.nlm.nih.gov/19411170/)
24. Garber ME, Wei P, KewalRamani VN, Mayall TP, Herrmann CH, Rice AP, et al. (1998) The interaction between HIV-1 Tat and human cyclin T1 requires zinc and a critical cysteine residue that is not conserved in the murine CycT1 protein. *Genes Dev* 12: 3512–3527. PMID: [9832504](https://pubmed.ncbi.nlm.nih.gov/9832504/)
25. Asamitsu K, Hibi Y, Imai K, Victoriano AF, Kurimoto E, Kato K, et al. (2011) Functional characterization of human cyclin T1 N-terminal region for human immunodeficiency virus-1 Tat transcriptional activation. *J Mol Biol* 410: 887–895. doi: [10.1016/j.jmb.2011.04.061](https://doi.org/10.1016/j.jmb.2011.04.061) PMID: [21763494](https://pubmed.ncbi.nlm.nih.gov/21763494/)
26. Asamitsu K, Hirokawa T, Hibi Y, Okamoto T (2015) Molecular dynamics simulation and experimental verification of the interaction between cyclin T1 and HIV-1 Tat proteins. *PLoS One* 10: e0119451. doi: [10.1371/journal.pone.0119451](https://doi.org/10.1371/journal.pone.0119451) PMID: [25781978](https://pubmed.ncbi.nlm.nih.gov/25781978/)
27. Jadowsky JK, Nojima M, Okamoto T, Fujinaga K (2008) Dominant negative mutant cyclin T1 proteins that inhibit HIV transcription by forming a kinase inactive complex with Tat. *J Gen Virol* 89: 2783–2787. doi: [10.1099/vir.0.2008/002857-0](https://doi.org/10.1099/vir.0.2008/002857-0) PMID: [18931076](https://pubmed.ncbi.nlm.nih.gov/18931076/)
28. Jadowsky JK, Nojima M, Schulte A, Geyer M, Okamoto T, Fujinaga K (2008) Dominant negative mutant cyclin T1 proteins inhibit HIV transcription by specifically degrading Tat. *Retrovirology* 5: 63. doi: [10.1186/1742-4690-5-63](https://doi.org/10.1186/1742-4690-5-63) PMID: [18620576](https://pubmed.ncbi.nlm.nih.gov/18620576/)
29. Verstraete N, Kuzmina A, Diribarne G, Nguyen VT, Kobbi L, Ludanyi M, et al. (2014) A Cyclin T1 point mutation that abolishes positive transcription elongation factor (P-TEFb) binding to Hexim1 and HIV tat. *Retrovirology* 11: 50. doi: [10.1186/1742-4690-11-50](https://doi.org/10.1186/1742-4690-11-50) PMID: [24985203](https://pubmed.ncbi.nlm.nih.gov/24985203/)
30. De Luca A, De Falco M, Baldi A, Paggi MG (2003) Cyclin T: three forms for different roles in physiological and pathological functions. *J Cell Physiol* 194: 101–107. doi: [10.1002/jcp.10196](https://doi.org/10.1002/jcp.10196) PMID: [12494448](https://pubmed.ncbi.nlm.nih.gov/12494448/)
31. Ramakrishnan R, Yu W, Rice AP (2011) Limited redundancy in genes regulated by Cyclin T2 and Cyclin T1. *BMC Res Notes* 4: 260. doi: [10.1186/1756-0500-4-260](https://doi.org/10.1186/1756-0500-4-260) PMID: [21791050](https://pubmed.ncbi.nlm.nih.gov/21791050/)
32. Zhou M, Halanski MA, Radonovich MF, Kashanchi F, Peng J, Price DH, et al. (2000) Tat modifies the activity of CDK9 to phosphorylate serine 5 of the RNA polymerase II carboxyl-terminal domain during human immunodeficiency virus type 1 transcription. *Mol Cell Biol* 20: 5077–5086. PMID: [10866664](https://pubmed.ncbi.nlm.nih.gov/10866664/)
33. Zhu Y, Pe'ery T, Peng J, Ramanathan Y, Marshall N, Marshall T, et al. (1997) Transcription elongation factor P-TEFb is required for HIV-1 tat transactivation in vitro. *Genes Dev* 11: 2622–2632. PMID: [9334325](https://pubmed.ncbi.nlm.nih.gov/9334325/)
34. Yang X, Herrmann CH, Rice AP (1996) The human immunodeficiency virus Tat proteins specifically associate with TAK in vivo and require the carboxyl-terminal domain of RNA polymerase II for function. *J Virol* 70: 4576–4584. PMID: [8676484](https://pubmed.ncbi.nlm.nih.gov/8676484/)
35. Gold MO, Yang X, Herrmann CH, Rice AP (1998) PITALRE, the catalytic subunit of TAK, is required for human immunodeficiency virus Tat transactivation in vivo. *J Virol* 72: 4448–4453. PMID: [9557739](https://pubmed.ncbi.nlm.nih.gov/9557739/)
36. Herrmann CH, Rice AP (1995) Lentivirus Tat proteins specifically associate with a cellular protein kinase, TAK, that hyperphosphorylates the carboxyl-terminal domain of the large subunit of RNA polymerase II: candidate for a Tat cofactor. *J Virol* 69: 1612–1620. PMID: [7853496](https://pubmed.ncbi.nlm.nih.gov/7853496/)
37. Ramakrishnan R, Dow EC, Rice AP (2009) Characterization of Cdk9 T-loop phosphorylation in resting and activated CD4(+) T lymphocytes. *J Leukoc Biol* 86: 1345–1350. doi: [10.1189/jlb.0509309](https://doi.org/10.1189/jlb.0509309) PMID: [19741158](https://pubmed.ncbi.nlm.nih.gov/19741158/)
38. Ramakrishnan R, Rice AP (2012) Cdk9 T-loop phosphorylation is regulated by the calcium signaling pathway. *J Cell Physiol* 227: 609–617. doi: [10.1002/jcp.22760](https://doi.org/10.1002/jcp.22760) PMID: [21448926](https://pubmed.ncbi.nlm.nih.gov/21448926/)
39. Russo AA, Jeffrey PD, Pavletich NP (1996) Structural basis of cyclin-dependent kinase activation by phosphorylation. *Nat Struct Biol* 3: 696–700. PMID: [8756328](https://pubmed.ncbi.nlm.nih.gov/8756328/)
40. Chen R, Yang Z, Zhou Q (2004) Phosphorylated positive transcription elongation factor b (P-TEFb) is tagged for inhibition through association with 7SK snRNA. *J Biol Chem* 279: 4153–4160. doi: [10.1074/jbc.M310044200](https://doi.org/10.1074/jbc.M310044200) PMID: [14627702](https://pubmed.ncbi.nlm.nih.gov/14627702/)
41. Ammosova T, Jerebtsova M, Beullens M, Lesage B, Jackson A, Kashanchi F, et al. (2005) Nuclear targeting of protein phosphatase-1 by HIV-1 Tat protein. *J Biol Chem* 280: 36364–36371. doi: [10.1074/jbc.M503673200](https://doi.org/10.1074/jbc.M503673200) PMID: [16131488](https://pubmed.ncbi.nlm.nih.gov/16131488/)
42. Ammosova T, Yedavalli VR, Niu X, Jerebtsova M, Van Eynde A, Beullens M, et al. (2011) Expression of a protein phosphatase 1 inhibitor, cdNIPP1, increases CDK9 threonine 186 phosphorylation and inhibits HIV-1 transcription. *J Biol Chem* 286: 3798–3804. doi: [10.1074/jbc.M110.196493](https://doi.org/10.1074/jbc.M110.196493) PMID: [21098020](https://pubmed.ncbi.nlm.nih.gov/21098020/)

43. Yang Z, Yik JH, Chen R, He N, Jang MK, Ozato K, et al. (2005) Recruitment of P-TEFb for stimulation of transcriptional elongation by the bromodomain protein Brd4. *Mol Cell* 19: 535–545. doi: [10.1016/j.molcel.2005.06.029](https://doi.org/10.1016/j.molcel.2005.06.029) PMID: [16109377](https://pubmed.ncbi.nlm.nih.gov/16109377/)
44. Mbyonye UR, Gokulrangan G, Datt M, Dobrowolski C, Cooper M, Chance MR, et al. (2013) Phosphorylation of CDK9 at Ser175 enhances HIV transcription and is a marker of activated P-TEFb in CD4(+) T lymphocytes. *PLoS Pathog* 9: e1003338. doi: [10.1371/journal.ppat.1003338](https://doi.org/10.1371/journal.ppat.1003338) PMID: [23658523](https://pubmed.ncbi.nlm.nih.gov/23658523/)
45. Tahirov TH, Babayeva ND, Varzavand K, Cooper JJ, Sedore SC, Price DH (2010) Crystal structure of HIV-1 Tat complexed with human P-TEFb. *Nature* 465: 747–751. doi: [10.1038/nature09131](https://doi.org/10.1038/nature09131) PMID: [20535204](https://pubmed.ncbi.nlm.nih.gov/20535204/)
46. D'Orso I, Jang GM, Pastuszak AW, Faust TB, Quezada E, Booth DS, et al. (2012) Transition step during assembly of HIV Tat:P-TEFb transcription complexes and transfer to TAR RNA. *Mol Cell Biol* 32: 4780–4793. doi: [10.1128/MCB.00206-12](https://doi.org/10.1128/MCB.00206-12) PMID: [23007159](https://pubmed.ncbi.nlm.nih.gov/23007159/)
47. Hornak V, Okur A, Rizzo RC, Simmerling C (2006) HIV-1 protease flaps spontaneously close to the correct structure in simulations following manual placement of an inhibitor into the open state. *J Am Chem Soc* 128: 2812–2813. doi: [10.1021/ja058211x](https://doi.org/10.1021/ja058211x) PMID: [16506755](https://pubmed.ncbi.nlm.nih.gov/16506755/)
48. Miller F, Kentsis A, Osman R, Pan ZQ (2005) Inactivation of VHL by tumorigenic mutations that disrupt dynamic coupling of the pVHL-hypoxia-inducible transcription factor-1alpha complex. *J Biol Chem* 280: 7985–7996. doi: [10.1074/jbc.M413160200](https://doi.org/10.1074/jbc.M413160200) PMID: [15611064](https://pubmed.ncbi.nlm.nih.gov/15611064/)
49. Toth G, Borics A (2006) Closing of the flaps of HIV-1 protease induced by substrate binding: a model of a flap closing mechanism in retroviral aspartic proteases. *Biochemistry* 45: 6606–6614. doi: [10.1021/bi060188k](https://doi.org/10.1021/bi060188k) PMID: [16716071](https://pubmed.ncbi.nlm.nih.gov/16716071/)
50. Filomia F, De Rienzo F, Menziani MC (2010) Insights into MAPK p38alpha DFG flip mechanism by accelerated molecular dynamics. *Bioorg Med Chem* 18: 6805–6812 doi: [10.1016/j.bmc.2010.07.047](https://doi.org/10.1016/j.bmc.2010.07.047) PMID: [20724167](https://pubmed.ncbi.nlm.nih.gov/20724167/)
51. Jin HX, Go ML, Yin P, Qiu XT, Zhu P, Yan XJ (2015) Determining the Functions of HIV-1 Tat and a Second Magnesium Ion in the CDK9/Cyclin T1 Complex: A Molecular Dynamics Simulation Study. *PLoS One* 10: e0124673. doi: [10.1371/journal.pone.0124673](https://doi.org/10.1371/journal.pone.0124673) PMID: [25909811](https://pubmed.ncbi.nlm.nih.gov/25909811/)
52. Asamitsu K, Omagari K, Okuda T, Hibi Y, Okamoto T (2016) Quantification of the HIV transcriptional activator complex in live cells by image-based protein-protein interaction analysis. *Genes Cells* 21: 706–716. doi: [10.1111/gtc.12375](https://doi.org/10.1111/gtc.12375) PMID: [27193293](https://pubmed.ncbi.nlm.nih.gov/27193293/)
53. Bowers KJ, Chow E, Xu H, Dror RO, Eastwood MP, Gregersen BA, et al. (2006) Scalable algorithms for molecular dynamics simulations on commodity clusters. *SC 2006 Conference, Proceedings of the ACM/IEEE Conference on Supercomputing*.
54. Victoriano AF, Okamoto T (2012) Transcriptional control of HIV replication by multiple modulators and their implication for a novel antiviral therapy. *AIDS Res Hum Retroviruses* 28: 125–138. doi: [10.1089/AID.2011.0263](https://doi.org/10.1089/AID.2011.0263) PMID: [22077140](https://pubmed.ncbi.nlm.nih.gov/22077140/)
55. Goh CS, Milburn D, Gerstein M (2004) Conformational changes associated with protein-protein interactions. *Curr Opin Struct Biol* 14: 104–109. doi: [10.1016/j.sbi.2004.01.005](https://doi.org/10.1016/j.sbi.2004.01.005) PMID: [15102456](https://pubmed.ncbi.nlm.nih.gov/15102456/)
56. Schulze-Gahmen U, Lu H, Zhou Q, Alber T (2014) AFF4 binding to Tat-P-TEFb indirectly stimulates TAR recognition of super elongation complexes at the HIV promoter. *Elife* 3: e02375. doi: [10.7554/eLife.02375](https://doi.org/10.7554/eLife.02375) PMID: [24843025](https://pubmed.ncbi.nlm.nih.gov/24843025/)